NON-LINEAR DARK CURRENT FIXED PATTERN NOISE COMPENSATION FOR VARIABLE FRAME RATE MOVING PICTURE CAMERAS

Michael Schöberl[1], Cihan Senel[2], Siegfried Fößel[2], Hans Bloss[2] and André Kaup[1]

[1]Multimedia Communications and Signal Processing
University of Erlangen-Nuremberg
Cauerstr. 7, 91058 Erlangen, Germany
{schoeberl, kaup} @lnt.de

[2]Fraunhofer Institute for Integrated Circuits IIS
Am Wolfsmantel 33, 91058 Erlangen, Germany

ABSTRACT

CMOS image sensors are used in most of the camera systems today. For achieving a high image quality it is essential to compensate for fixed pattern noise. Compensation can be carried out by subtracting an estimated noise value per pixel, either directly on the sensor or in the digital processing. Unfortunately these values are different for each camera and will vary for different exposure times, camera mode settings and temperature. This poses additional challenges for high-end moving picture camera systems. We present a new algorithm for improved fixed pattern noise compensation that extends the currently available linear models. Measurements of a real world camera system and a simulation are used to show the improvements with our algorithm. Significant improvement of the compensated fixed pattern noise over a wide exposure range is shown. This allows the operation of the camera system at a much wider range of frame rates and especially long exposures are now possible. Our algorithm can be implemented without increasing the required memory bandwidth which saves power, size and cost.

1. INTRODUCTION

With todays CMOS sensors a high image quality is possible. Their low power consumption and cost made them popular for a low end mass market like mobile phone cameras. This fueled the research and even better high-end CMOS sensors are available today. Still, the images from a CMOS sensor suffer from various distortions and image processing for the removal of noise is necessary for obtaining high quality images. The signal processing for removing the noise works reliably as most of the noise is predictable.

This fixed pattern noise is mostly caused by inhomogenity in the manufacturing of the silicon sensor. Tiny variations in size, position or temperature of a transistor result in slightly different characteristic. The analog operation of the transistors of an active pixel sensor and their non-ideal behavior result in the degradation of the image. Extensive sensor cooling as in astro photography [6] as well as improvements in sensor technology [1] both help to reduce fixed pattern noise. This certainly improves image quality but does not release the high-end market from compensation algorithms. Even then additional improvements can be achieved with compensation algorithms (see example in Figure 1).

For high-end motion picture camera systems an instant compensation for all possible exposure times is required. The user needs to be able to select from different exposure times without a time consuming re-calibration. The exposure time could even change while the camera is running. While ”overcranking” the camera runs faster than playback and a slow motion effect is achieved. A seemless transition of the exposure time needs to be performed.

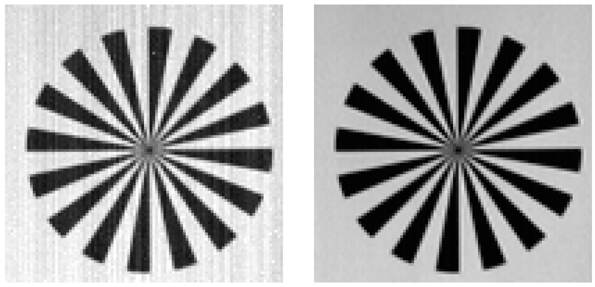

a) b)

Figure 1: Noise removal image processing: a) uncompensated image with fixed pattern noise, b) after compensation

Various methods for fixed pattern noise reduction have been suggested: The most basic idea captures and stores a dark frame and later subtracts it from a regular bright frame [5]. This method is directly applied in astro photography and some of the still photography cameras today. It does not work for a continuous operation of a camera with variable exposure time.

The model in [3] distinguishes only offset noise for columns and single pixels. This helps in characterizing the silicon structure but gives no advantage over [5] for compensation of a single pixel. In [2] a setup for gain FPN calibration is shown. A model for dark current FPN compensation with variable exposure time has been proposed in [9]. Our simulation shows that this linear model works well on average. Still, a visually disturbing noise pattern remains as the non-linear behaviour of a small percentage of pixels can not be compensated. In the field of semiconductor image sensor design more complex FPN models are used for the analysis of design decisions [4]. Unfortunately they are too complex for a real time compensation. FPN compensation models also exist for high dynamic range logarithmic image sensors [8] but these models are not applicable to linear image sensors. The calibration of [7] is used for temperature variations of offset and gain in CCD image sensors. The specific problem of dark current is not adressed there.

This paper starts with an image formation model that distinguishes different types of CMOS image sensor noise. We show measurements of a real world camera system in Section 3. One existing linear [9] and two new non-linear fixed pattern noise models are then shown in Section 4. Calibration procedures are explained accordingly. The models are then compared in a simulation in Section 5.

© EURASIP, 2009

2. IMAGE FORMATION MODEL

When capturing an image there are many components that show non-ideal behavior. This leads to severe image degradation which can be described as noise. Our analysis describes the behavior for a single and independent pixel, and the description thus omitts the pixel position (x,y). We want to specifically distinguish between two types of noise for each pixel:

$$I = \tilde{I} + N_{\text{fixed}} + N_{\text{dynamic}} \tag{1}$$

The static or fixed pattern noise N_{fixed} desribes distortions that can in some way be predicted. This does not mean that they are fixed in general but that their dependencies are well understood. These dependencies on temperature or exposure time can then be controlled (e.g. with temperature stabilization) or measured and accurate noise predictions can be made. A subtraction of the fixed noise then leads to an improvement in image quality [5]. In general we can distinguish three major contributions:

$$N_{\text{fixed}} = N_{\text{offset}} + N_{\text{dark}} + N_{\text{prnu}} \tag{2}$$

The offset N_{offset} is caused by semiconductor variations. It varies with temperature T but is independent otherwise. The dark current N_{dark} is caused by a leakage current and a pixel will ”fill up” even without any light. It depends on the exposure time τ_{exp} and the sensor temperature T. Examples for typical N_{offset} and N_{dark} patterns can be seen in Figure 2. Each pixel has a slightly different sensitivity which is commonly called ”Photo Response Non Uniformity” noise N_{prnu}. It is caused by variations in size and position of the photo site electronics and depends on the amount of light I. A model as shown in [2] assumes a fixed multiplicative gain G per pixel. The additive noise can then be written as

$$N_{\text{prnu}} = (G-1)\cdot\tilde{I} \tag{3}$$

In the following analysis we want to concentrate on N_{fixed} which is especially disturbing in dark image areas. The PRNU noise is insignificant in these image areas and $N_{\text{prnu}} \approx 0$ is used throughout this paper.

The temporal dynamic noise N_{dynamic} changes from one frame to another. It is caused by many effects within the photo site and sensor readout. This includes reset noise, photon shot noise, readout noise, quantization noise and dark current shot noise [10]. We assume an uncorrelated zero mean dynamic noise. We might be able to model and predict its statistics but the values itself are unknown. A reduction by subtraction of an estimate is not possible.

3. MEASUREMENTS OF A REAL WORLD SYSTEM

For evaluating the quality of the compensated images we need to compare them based on real world data from a camera. We set up a measurement that delivers dark current for many exposure times. This can be used for the calibration of our models as well as the evaluation of the quality of the models (see below).

3.1 Experimental Setup

We used a high resolution (6 MPixel) photodiode active pixel sensor with 8.25 um pixels. Sampling was done with 12 Bits of resolution. To avoid drift we used a temperature stabilized

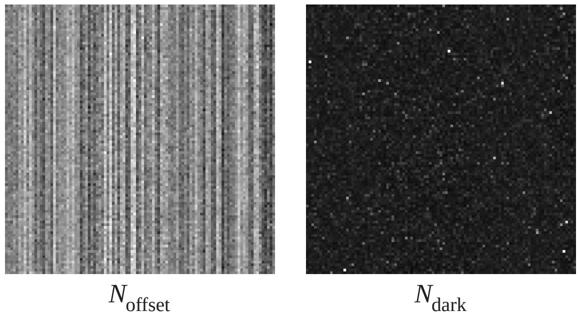

Figure 2: Typical fixed pattern noise components, $\tau_{\text{exp}} =$ 100 ms, displayed with a gain of x16

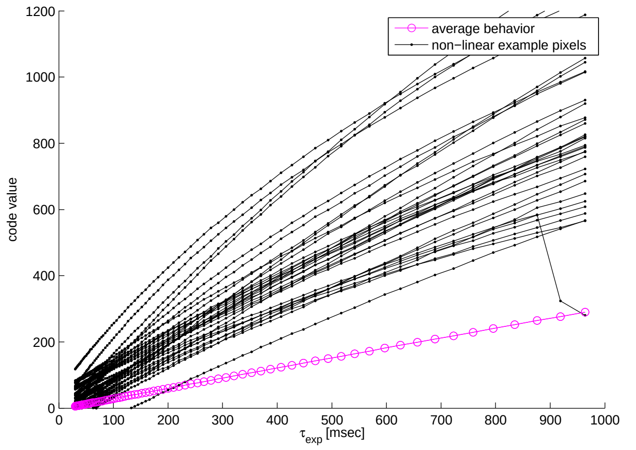

Figure 3: Measured dark current N_{dark} on average and examples for non-linear pixels

sensor system. The temperature of the camera system was kept constant as well. The sensor was covered and all of the camera system was shielded from light.

For each exposure time we captured $M = 15$ pairs of frames with $\tau = \tau_{exp}$ and $\tau = 0$ over the range of exposure times from 30 ms to 1 sec. The captured information of a single pixel of the kth frame with exposure time τ is denoted by $I_k(\tau)$. The analysis is shown for many independent pixels.

3.2 Measurement Results

From the captured pixel values $I_k(\tau)$ we can calculate average values for each pixel and exposure time:

$$\bar{I}(\tau) = \frac{1}{M}\sum_{k=0}^{M-1} I_k(\tau) \tag{4}$$

From this data we can calculate the dark current noise N_{dark} for each pixel. According to our image formation model we can use

$$N_{\text{dark}}(\tau_{\text{exp}}) = \bar{I}(\tau_{\text{exp}}) - \bar{I}(0) \tag{5}$$

The dark current noise average across all pixels of the image is shown in Figure 3. We can see that on average the dark current noise rises linear with exposure time. On average pixels can be assumed to have a constant dark current i_{dark} which can be represented by the linear model.

Measurements have shown that there are over 1 % of pixels that show a non-linear behavior. Some examples of these pixels can also be seen in Figure 3. The overall number of pixels with non-linear behavior is large and we should not classify all of these pixels as "dead". Although they follow a non-linear behavior over exposure time they are still sensitive to light and can contribute to the final image. A reduced dynamic range for these pixels needs to be kept in mind.

3.3 General Validity

The reasons for this behavior of the photo site lie in the leakage current which depends on the remaining reverse voltage across the photo diode [4]. We were able to measure the same behavior for different types of CMOS sensors.

The reverse voltage will also change if the sensor sees light. The models and assumptions will be inaccurate for high amounts of light and are only useful for a medium to low range of light. As the dark current and offset noise are only visible in low light situations anyway, these models are still useful for this range. With a high amount of light the photon shot noise dominates the dynamic noise and dark current fixed pattern noise effects will be less visible.

4. FPN COMPENSATION MODELS

For compensating the fixed pattern noise N_{fixed} we need to find estimates for its components. These components can then be subtracted from the image. We will show an existing linear and two new models to estimate these components for offset and dark current noise for each pixel of the image. Furthermore we asume a stabilized temperature for sensor and analog electronics.

Although these models do not seem to be overly complex, one needs to be aware that they need to be evaluated for every pixel of every frame. This limits the number of operations as well as the number of parameters for a real-time implementation. Exponential dark current models like [4] are too complex for a real time image compensation.

4.1 Linear Model

The model in [9] assumes a dark current i_{dark} that is constant for each pixel (see Figure 4). This leads to a linear compensation algorithm that calculates the fixed pattern noise with

$$N_{\text{fixed}} = i_{\text{dark}} \cdot \tau_{\text{exp}} + N_{\text{offset}} \tag{6}$$

For the calibration of the camera system a set of two exposures with exposure times $\tau = \tau_{\text{exp}}$ and $\tau = 0$ can be used. The per-pixel dark current can then be estimated by

$$i_{\text{dark}} = \frac{1}{\tau_c} \left[\bar{I}(\tau_c) - \bar{I}(0)\right] \tag{7}$$

$$N_{\text{offset}} = \bar{I}(0) \tag{8}$$

The selection of the calibration point τ_c depends on the application. For exposure times close to the calibration the error will be lower.

4.2 Segmented Linear Model

Our measurements have shown that although the linear model works well on average, there are some outliers. These pixels follow a non-linear behavior and are not well represented with the above model. Unfortuately they are visually disturbing and need to be taken care of.

We propose a model that consists of N segments. Within these segments we use a linear model. The segment boundaries are defined by the exposure times with segment n lying between τ_{n-1} and τ_n. An example with $N = 3$ can be seen in Figure 5. For each pixel we use a set of independent parameters i_n and O_n. The same segment borders τ_n are used for all pixels of an image. The compensation can be carried out with this equation:

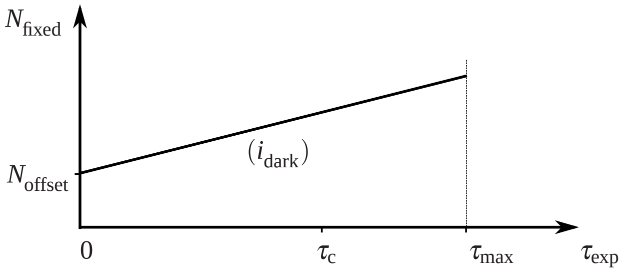

Figure 4: Linear model for FPN compensation

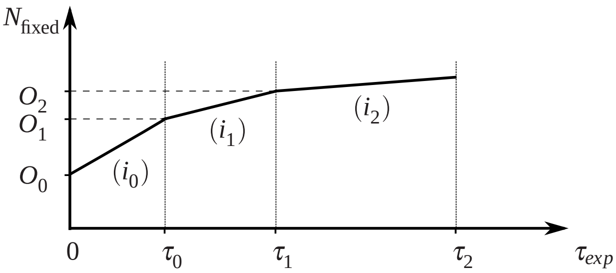

Figure 5: Segmented linear model for FPN compensation

$$N_{\text{fixed}} = \begin{cases} i_0 \cdot \tau_{exp} + O_0 & \text{if } n = 0 \\ i_n \cdot (\tau_{exp} - \tau_{n-1}) + O_n & \text{else} \end{cases} \tag{9}$$

This algorithm requires additional memory for storing the parameters i_n and O_n for each segment. The size of todays memory chips makes this easily possible. The data rate on the other hand is not increased as for a single image we only need to read i_n and O_n from memory. The decision about the segment is done based on the exposure time τ_{exp} only once per image.

The calibration of a camera with this model estimates the parameters i_n and O_n. For each segment we need to observe an averaged set of frames. The first segment can directly be calibrated like a linear model:

$$i_0 = \frac{1}{\tau_0} \left[\bar{I}(\tau_0) - \bar{I}(0)\right] \tag{10}$$

$$O_0 = \bar{I}(0) \tag{11}$$

For the following segments we assign

$$i_n = \frac{1}{\tau_n - \tau_{n-1}} \left[\bar{I}(\tau_n) - O_{n-1}\right] \tag{12}$$

$$O_n = i_{n-1} \cdot \tau_{n-1} + O_{n-1} \tag{13}$$

Minor error might occur due to rounding the values for a fixed point implementation. This calibration procedure still guarantees a continuous dark current representation without adding up the errors.

The segmented model can also be used with a correlated double sampling sensor mode. This will deliver a reduced reset noise and cancellation of the offset noise. The calibration can be carried out as shown above with the result of

$$O_0 = \bar{I}(0) - \bar{O}_{\text{CDS}} \approx 0 \tag{14}$$

4.3 Quadratic Model

For comparison of non-linear models we also used a model based on a quadratic polynom as shown in Figure 6. This requires three parameters and two additional multiplications per pixel:

$$N_{\text{fixed}} = a \cdot \tau_{exp}^2 + b \cdot \tau_{exp} + c \tag{15}$$

The per pixel parameters a, b and c can be calculated by fitting a polynom to measurements $\bar{I}(\tau)$ with at least 3 different exposure times.

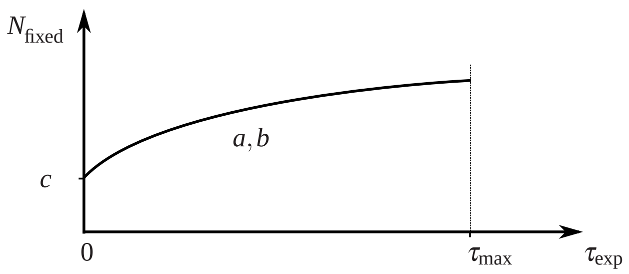

Figure 6: Quadratic model for FPN compensation

5. EXPERIMENTAL RESULTS

For evaluating the performance of the algorithms we performed an offline compensation for the measured real world data. Only few (see below) of the measured data points were used to calculate the compensation parameters for all pixels and models. For the remaining samples we then performed the compensation. Fitting the models to many more data points could further reduce the error but is clearly impractical for a real world calibration of camera systems.

For the linear model we used $\tau_c = 750$ msec to calibrate the model. This gives a low average error but generates a good compensation only for this exposure time. Calibrating for a typical exposure time of e.g. $\tau_c = 30$ msec is desirable for typical operation modes but this would lead to even worse compensation for long exposure times. We can clearly see the limits of a linear model.

For the segmented model we chose $N = 4$ which is still practical for an implementation and gives reasonable compensation quality. We used the segment borders $\tau_0 = 65$ msec, $\tau_1 = 257$ msec, $\tau_2 = 590$ msec and $\tau_2 = 955$ msec.

For the quadratic model we used the same 5 data points and fitted a polynomial model of order 2 with the Matlab `polyfit` function.

In Figure 7 we can see the resulting error over exposure time for all pixels from an example region of the image. The first row shows the mean error for each exposure time. We can see that the error for bad pixels is reduced compared to the linear model. The second row shows error histograms and the average error as well as the outliers are significantly reduced. These outliers are visually disturbing and prevented the use of a linear compensation for a large range of exposure times. This is confirmed by looking at the third row. It shows the remaining fixed pattern noise for an exposure time of $\tau_{\text{exp}} = 100$ msec. Especially the few but disturbing pixels are reduced. For a numeric comparison of the algorithms the mean and variance of the compensated images is shown in Table 1. We can see that our segmented method reduces both the mean error and variance by a factor of over 3 compared to the linear compensation.

Method	mean error	variance
Linear	0.90	5.70
Segmented linear	0.27	1.50
Quadratic	0.29	1.89

Table 1: Remaining image noise (mean and variance) for simulated compensation, average over all exposure times

For this system we measured the average dynamic noise variance to $N_{\text{dynamic}} = 1.88$. Both the segmented and quadratic approach can reduce the fixed noise below this level. In contrast to the linear compensation both of these methods will be able to generate compensated images where a fixed pattern noise is not noticable any more. The few remaining pixels that will still be visible can now be classified as dead pixels.

This increased compensation quality is possible without additional memory bandwidth which is currently the limiting factor in mobile camera systems. The additional storage for a 6 MPixel camera amounts to only 75 MBytes, which is easily available with current memory ICs. The number of additional computations is small and typical camera implementations can easily be adjusted. This leads to a larger usable range of exposure times without increasing the cost of a camera system.

6. CONCLUSIONS

We show measurements of the fixed pattern noise behavior of a real world CMOS sensor. Specifically the non-linear dark current of some of the pixels is analyzed.

Based on the observed non-linearities we extend existing linear dark current compensation models with a new non-linear model. We propose a segmented linear compensation that allows a wide range of exposure times. We also show the calibration computations that guarantee a continuous model even with rounding necessary in fixed point implementations.

We compare the models based on a simulated compensation which is based on measured dark current behavior and a calibration of the models. Results for the compensation quality are shown and the real-time implementation requirements are analyzed. The new segmented model is able to both reduce the average compensation error as well as the variance by a factor of 3. The error reduction of outliers is especially important as these pixels are highly visible in the final image. For our system we can reduce the fixed pattern noise below the dynamic noise which is essential for using the camera modes.

Our model enables the compensation quality of a quadratic model without increasing the hardware resources compared to a linear model. This reduces the hardware costs for a camera system and enables an increased image quality. This enables additional camera modes with longer exposure times and a high image quality without further increasing the cost of the system.

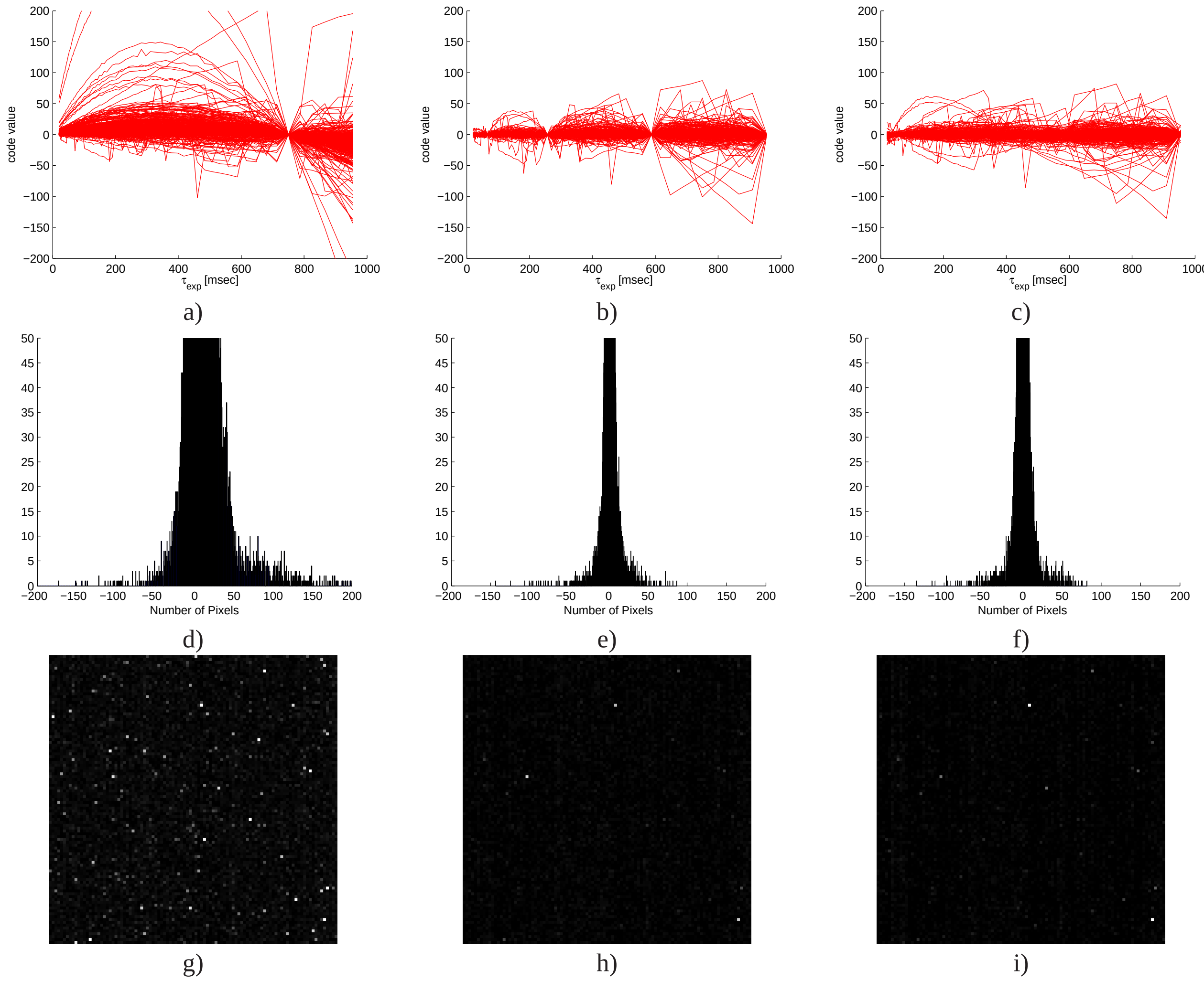

Figure 7: Simulated compensation error for linear (left a), d), and g)), segmented linear (center b), e) and h)) and quadratic model (right c), f) and i)). The mean compensation error over exposure time is shon in a), b) and c), overall error histograms can be seen in d), e) and f) and g), h), and i) show the remaining noise in compensated image areas (gain of x128, $\tau_{exp} = 100$ msec)

REFERENCES

[1] M. Bigas, E. Cabruja, J. Forest, and J. Salvi. Review of CMOS Image Sensors. *Microelectronics Journal*, 37(5):433 – 451, 2006.

[2] B. Fowler, A. E. Gamal, D. Yang, and H. Tian. A Method for Estimating Quantum Efficiency for CMOS Image Sensors. In *SPIE Solid State Sensor Arrays: Development and Applications II*, volume 3301, pages 178–185. SPIE, 1998.

[3] A. E. Gamal, B. A. Fowler, H. Min, and X. Liu. Modeling and estimation of FPN components in CMOS image sensors. In *SPIE Solid State Sensor Arrays: Development and Applications II*, volume 3301, pages 168–177. SPIE, 1998.

[4] N. Loukianova, H. Folkerts, J. Maas, D. Verbugt, A. Mierop, W. Hoekstra, E. Roks, and A. Theuwissen. Leakage Current Modeling of Test Structures for Characterization of Dark Current in CMOS Image Sensors. *IEEE Transactions on Electron Devices*, 50(1):77–83, Jan 2003.

[5] R. Malueg. Detector Array Fixed-Pattern Noise Compensation, Apr. 6 1976. US Patent 3,949,162.

[6] I. McLean. *Electronic Imaging in Astronomy. Detectors and Instrumentation*. Wiley-Praxis Series in Astronomy and Astrophysics. John Wiley and Sons, 1997.

[7] J. Newman. Method and Apparatus for Image Signal Compensation of Dark Current, Focal Plane Temperature, and Electronics Temperature, June 26 2007. US Patent 7,235,773.

[8] S. Otim, D. Joseph, B. Choubey, and S. Collins. Modelling of High Dynamic Range Logarithmic CMOS Image Sensors. *Proceedings of the 21st IEEE Instrumentation and Measurement Technology Conference IMTC04*, 1:451–456, May 2004.

[9] B. Pillman, R. Guidash, and S. Kelly. Fixed Pattern Noise Removal in CMOS Imagers Across Various Operational Conditions, Aug. 15 2006. US Patent 7,092,017.

[10] H. Tian, B. A. Fowler, and A. E. Gamal. Analysis of temporal noise in CMOS APS. In *SPIE Sensors, Cameras, and Systems for Scientific/Industrial Applications*, volume 3649, pages 177–185. SPIE, 1999.